Optimal Paths in Still Air for a Sailplane with a Quadratic Glide Polar

Artur Wolek and Craig Woolsey
artur.wolek.ctr@nrl.navy.mil,cwoolsey@vt.edu
Virginia Tech, Blacksburg, VA

Abstract

This paper considers the optimal control problem of minimizing the altitude loss of a glider maneuvering in still air to a nearby position and heading angle under shallow bank angle assumptions. The glider's motion, as viewed from above, is modeled as a kinematic car with control inputs of forward speed and turn rate. (In practice, a glider can adjust its flight path angle and bank angle to achieve a desired forward speed and turn rate.) The speed control is strictly positive, varying from the stall speed to the maximum speed, and the turn rate is symmetrically bounded about zero. The sink rate of the glider is assumed to be a quadratic function of the forward speed, approximating the "glide polar". Necessary conditions derived from the Minimum Principle are used to characterize the extremal controls. Further, suboptimality conditions are identified geometrically to arrive at a finite and sufficient set of candidate optimal controls. The extremal paths are shown to consist of (i) straight line segments flown at the glider's "best glide" speed and (ii) maximum rate turns with either: (a) a heading dependent speed input, (b) the stall speed, or (c) the minimum sink speed. A synthesis procedure is proposed to solve for the optimal path. These results may be applicable to autonomous sailplanes or manned aircraft experiencing loss of thrust (under autopilot control).

Introduction

This paper concerns optimal maneuvering of a sailplane between nearby positions and heading angles with minimal loss of altitude. The length scale of interest is on the order of a few turning radii of the glider. The minimum turning radius and the sink rate depend on the airspeed in gliding flight, and there is a tradeoff between turn radius and altitude loss. (At slower speeds the glider can turn more sharply, but with an increased sink rate.) In this work, an optimal control problem is formulated that approximately captures this tradeoff – we model the glider as a planar kinematic car with speed and turn rate controls, a sink rate that is a quadratic function of the speed, and a minimum turn radius that scales linearly with the speed.

Previous work concerning glider path optimization has largely focused on how to make the most effective use of available sources of lift (such as thermals, ridge lift, lee waves, etc.) along a flight route. Flight between thermals for given wind conditions has been studied to determine optimal equilibrium flight speeds [1, 2] and optimal transient motions for leaving and entering a thermal [3, 4]. Further, the use of various flight techniques, such as dolphin-style soaring (traversing thermals without circling) [5, 6] or essing maneuvers (alternating partial left and right turns while traversing thermals) [7], has been studied extensively. Stochastic optimal control techniques have been used to address the problem of gliding with uncertain knowledge of future lift conditions [8–10]. Graph-based approaches have been used to compute energy optimal sailplane routes [11]. In most cases, the path optimization problem is constrained to the vertical plane and the turning motions of the sailplane are ignored.

On the scale of cross-country soaring, the negligible effect of turning motions may justify ignoring them. However, optimal turns become important over small distances when there are no sources of lift (still air) and the altitude loss to a desired position and heading can only be minimized by careful maneuvering. This is the setting for the present study. An autonomous sailplane may take advantage of these results to perform short maneuvers that reposition the glider relative to a thermal, change course angle, avoid obstacles, or align with the runway for a landing approach.

Past work most relevant to this study relates to emergency landing paths for powered aircraft experiencing a loss of thrust. At a low altitude after experiencing a loss of thrust during climb-out, civil aviation authorities recommend selecting a landing site within a 60 degree heading angle downrange from the point of failure [12]. Alternatively, one encounters the so called "impossible turn" problem [13] where the task is to maneuver with minimum altitude loss and return to the runway safely. Ignoring transient motions, it has been shown that the steady-state optimal path, in this case, is tear-drop shaped, consisting of a 45-degree bank angle turn at the stall speed, followed by a best glide slope straight segment [13]. Related studies have considered the prob-

lem of maximizing range in a given direction (that is, parallel to but not necessarily coincident with the runway) [14], or optimizing the turnback maneuver to the nearest point along the runway [15]. However, in all of these studies, the final endpoint is not fully constrained and hence the boundary conditions differ from the problem considered here. (We assume the terminal position and heading angle are given.) If an aircraft experiences loss of thrust at a high enough altitude then it may be able to perform a wider range of turning motions safely and there may be several suitable landing sites to consider (rather than restricting the search for a landing site to areas directly downrange, as previously discussed). The emergency landing problem then requires planning a path to each candidate landing site and comparing the associated altitude loss with each path. This case is perhaps the most relevant to the present work, since the boundary conditions and the objective are the same – to glide to a desired point with a specified approach angle while minimizing altitude loss. Graph-based approaches are particularly useful to determine the landing trajectory when obstacles are present [16]. In the absence of obstacles, the reliable and computationally efficient Dubins path planning approach [17] has been proposed to quickly compare several landing sites [18, 19]. In [20], emergency flight paths are computed using a modified Dubins parameterization that incorporates acceleration, variable turn rate, constant wind conditions, and rate limits on bank angle. (Dubins path planning gives a simple geometric way to construct minimum length paths of bounded curvature. These consist of straight segments and circular arcs. This planning approach has been widely used for guidance of aircraft [21] and planar robots [22, 23]. It has also been extended to account for various wind conditions [24–26] or for the motion of an aircraft with a damaged steering mechanism [27, 28].)

Last, we note that another related problem concerns the deployment of a glider to a desired point, with a free heading angle, while maximizing endurance [29, 30]. This problem was considered in the context of a military aircraft deploying a gliding weapon, wherein the goal was to maximize the time to impact the target so that the aircraft can escape to safety. In this case, however, the cost function is not equivalent to maximum range and the boundary conditions differ from those we consider.

In the present study, we assume a similar kinematic car model as in [18, 19], however we relax the fixed speed constraint and consider a cost function derived from the glide polar. One advantage of this formulation is that it becomes tractable to solve the optimal control problem using the indirect method. (That is, we may apply the Minimum Principle and study the resulting necessary conditions for optimality.) This allows us to analytically characterize the structure of the optimal control and gain greater insight into the problem. (Alternatively, relying on direct methods that discretize the problem, one obtains a numerically approximate solution that may inform one's understanding of optimal paths.) The disadvantage, of course, is that the sailplane dynamics have been approximated, using the kinematic car and quadratic sink rate model, and the solution is only as good as this approximation. We view the present study as an exercise aimed at gaining new insight regarding optimal paths for a glider maneuvering in still air.

Properties of the Glide Polar

The objective is to minimize the change in altitude while steering a glider to a desired position in the horizontal plane (viewed from above) and with a desired final heading angle. The control inputs are horizontal speed v and turn rate u. The sink rate is often expressed as a function of the glider's speed using the so-called "glide polar" plot, sketched in Fig. 1. The glide polar illustrates the relationship between horizontal speed v and sink rate w for a glider in steady flight in still air. (In the presence of horizontal or vertical winds the glide polar can be adjusted accordingly.) The angle between the horizontal axis and the ray emanating from the origin to a point (v,w) along the curve gives the corresponding flight path angle γ. Several important flight conditions are labeled on the glide polar in Fig. 1: the "stall speed" v_{stall}, the "minimum sink" speed v_{ms}, the "speed to fly" v_{stf} and the maximum speed $v_{\max}$.

Flying in a straight line at the minimum sink speed v_{ms} gives the lowest sink rate and will minimize the loss of altitude per unit time; this speed will maximize endurance. However, an observation well known to sailplane pilots [1] is that flying faster, at the speed to fly v_{stf} (also called the "best glide speed" or the "best L/D speed" where L/D is the lift to drag ratio), maximizes range per unit altitude and minimizes the flight path angle γ. Note that the term "speed to fly" is used to refer to the optimum airspeed in a more general class of optimization problems (such as maximizing cross-country speed for various wind and thermal conditions). However, in this work we use the term to strictly refer to the best glide speed in still air. The following assumptions are made about the glide polar:

Assumption 1. *The glide polar is given by* $w(v) = av^2 + bv + c$, *where* $a > 0$, $v \in [v_{\text{stall}}, v_{\max}]$ *and* $w(v) > 0$.

Similar assumptions of a quadratic glide polar are often made in the literature [31]. The coefficients a, b and c characterize a

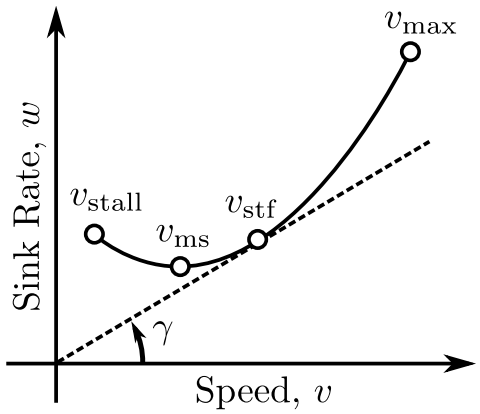

Fig. 1: A typical glide polar

particular sailplane's sink rate as a function of airspeed in still air. The range of $w(v)$ excludes the possibility of a zero sink rate and the assumption that $a > 0$ implies that $w(v)$ is convex. We assume that the stall speed $v_{\text{stall}} > 0$.

Assumption 2. *The minimum sink speed occurs at the critical point* $v_{\text{ms}} \in (v_{\text{stall}}, v_{\text{max}})$.

The critical point of $w(v)$ occurs at $v_{\text{ms}} = -b/2a$ so that $w(v_{\text{ms}}) = -b^2/4a + c$. Since $v_{\text{ms}} > 0$ and $w(v) > 0$ is required, it follows that $b < 0$ and $c > b^2/(4a)$.

Assumption 3. *The speed to fly occurs at* $v_{\text{stf}} \in (v_{\text{stall}}, v_{\text{max}})$.

The speed to fly is the point along the glide polar where the tangent line to the polar passes through the origin [1, 32] as shown in Fig. 1; equivalently, it is the speed at which $\frac{d}{dv}w(v) = w(v)/v$. Given the previous assumptions, this condition is satisfied at $v_{\text{stf}} = \sqrt{c/a}$ with $v_{\text{stf}} > v_{\text{ms}}$.

Assumption 4. *The minimum sink speed occurs at least half way between the stall speed and the speed to fly:* $v_{\text{ms}} > (v_{\text{stall}} + v_{\text{stf}})/2$

This condition is a simplifying assumption used in the derivation of the extremal controls. In the example case considered later in this work it is shown that this is a reasonable assumption, however not all glide polars will satisfy this condition.

Remark 1. *Typically, there is no experimental data for gliders in turning flight. However, it is possible to estimate the sink rate in a turn from level flight polar data as discussed in [33]. Alternatively, one might derive the sink rate as a function of both the turn rate (or the load factor) and speed* $w(u,v)$ *by considering a performance model of a glider subject to aerodynamic, gravitational, and inertial forces [34]. In this work we assume that the sink rate* $w(v)$ *is independent of the turn rate u, recognizing that this may only hold for shallow turns.*

Problem Formulation

Consider the projected planar motion of a glider (as viewed from above) where $(x,y) \in \mathbb{R}^2$ is the planar position of the vehicle and $\psi \in [0, 2\pi)$ is its heading, as shown in Fig. 2. The equations of motion for this model with speed v and turn rate u controls are:

$$\dot{x}(t) = v(t)\cos\psi(t) \tag{1}$$
$$\dot{y}(t) = v(t)\sin\psi(t) \tag{2}$$
$$\dot{\psi}(t) = u(t) \tag{3}$$

The turn rate control is symmetrically bounded $u \in [-u_{\text{max}}, u_{\text{max}}]$. The speed control interval is strictly positive $v \in [v_{\text{stall}}, v_{\text{max}}]$ with $v_{\text{stall}} > 0$. The control input function is then $\mathbf{u}(\cdot) = (u(\cdot) \quad v(\cdot))^{\text{T}}$. Assuming quasi-steady flight, we define the cost functional $J(\mathbf{u}(\cdot))$ as the integral of the sink rate $w(v)$ to give the total altitude loss:

$$J(\mathbf{u}(\cdot)) = \int_{t_0}^{t_1} \left(av(\sigma)^2 + bv(\sigma) + c\right) d\sigma \tag{4}$$

Let the boundary conditions include the initial state $\mathbf{x_0} = (0 \quad 0 \quad 0)^{\text{T}}$ and an initial time t_0, and the terminal state $\mathbf{x_1} = (x_1 \quad y_1 \quad \psi_1)^{\text{T}}$ and some unknown final time $t_1 > t_0$. Define the control constraint set

$$\Omega = \{(u,v) \mid v_{\text{stall}} \le v \le v_{\text{max}} \text{ and } |u| \le u_{\text{max}}\} \tag{5}$$

Denote the set of real n-dimensional vectors of piecewise continuous functions on the interval $[t_0, t_1]$ as $PWC(t_0, t_1; \mathbb{R}^n)$. Then the set of piecewise continuous admissible controls that satisfy the boundary conditions is

$$\Theta = \left\{ \begin{array}{c} \mathbf{u}(\cdot) \in PWC(t_0, t_1; \mathbb{R}^2) : \mathbf{u}(t) \in \Omega \\ \text{except at a finite number of points} \\ \text{and } \mathbf{u}(\cdot) \text{ steers } \mathbf{x_0} \text{ to } \mathbf{x_1} \end{array} \right\}$$

The problem is to find an optimal control $\mathbf{u}^*(\cdot) \in \Theta$ such that $\mathbf{u}^*(\cdot)$ steers $\mathbf{x_0}$ to $\mathbf{x_1}$ at $t_1 \ge t_0$ with $J(\mathbf{u}^*(\cdot)) \le J(\mathbf{u}(\cdot))$ for all $\mathbf{u}(\cdot) \in \Theta$.

Controllability and Existence of an Optimal Control

The "Dubins car" problem [17] satisfies the same state equations (1)-(3) as the problem considered here, but with a constant speed constraint and a cost functional for minimum time. Since it has already been established that the Dubins car is controllable [17], it follows that the system considered here is also controllable. An optimal control exists for a system in the form $\dot{\mathbf{x}} = \vec{f}(\mathbf{x}, \mathbf{u})$ with a Hamiltonian that is strictly convex in the controls (assuming $\vec{f}(\mathbf{x}, \mathbf{u})$ satisfies certain continuity and boundedness assumptions). Referring to Ref. 35, one can verify that these conditions are satisfied by the system considered here, therefore an optimal control exists.

Applying the Minimum Principle

The Minimum Principle provides necessary conditions for an optimal control. For an in-depth discussion, the reader can refer

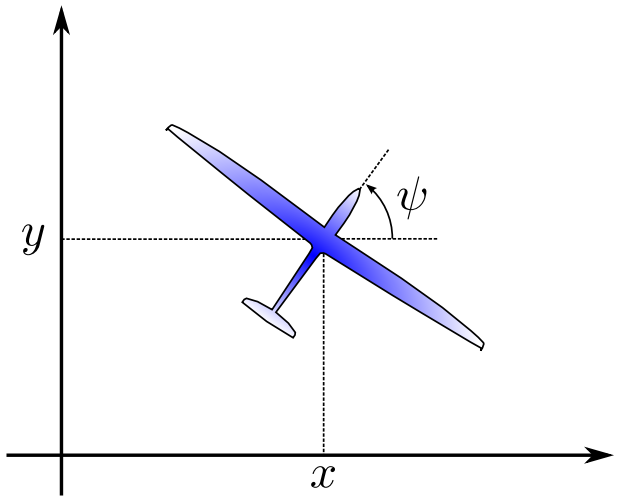

Fig. 2: The state of the glider model is its planar position (x,y) **and heading** ψ

to one of the standard texts [36–38]. To apply the Minimum Principle, we introduce the variational Hamiltonian

$$\begin{aligned} H &= \eta_0 w(v) + \langle \vec{\eta}, \vec{f}(\psi,u,v)\rangle \\ &= \eta_0\left(av^2+bv+c\right) + v(\eta_x\cos\psi + \eta_y\sin\psi) + \eta_\psi u \end{aligned}$$

where $\vec{f}(\psi,u,v)$ is the right hand side of the state-system (1)-(3) and $\vec{\eta} = (\eta_x\ \eta_y\ \eta_\psi)^T$ is a vector of corresponding adjoint variables. (The explicit time dependence of the variables is suppressed for brevity.) Also, $w(v)$ is the integrand of the cost-functional (4) and η_0 is the associated adjoint variable. The Minimum Principle states that if a control pair (u^*,v^*) is optimal, then there exists a constant $\eta_0 \geq 0$ and absolutely continuous functions $\eta_x(\cdot)$, $\eta_y(\cdot)$ and $\eta_\psi(\cdot)$ such that

$$\dot{\eta}_x(t) = -\frac{\partial H}{\partial x} = 0 \tag{6}$$

$$\dot{\eta}_y(t) = -\frac{\partial H}{\partial y} = 0 \tag{7}$$

$$\dot{\eta}_\psi(t) = -\frac{\partial H}{\partial \psi} = v(t)(\eta_x\sin\psi(t) - \eta_y\cos\psi(t)) \tag{8}$$

(Note that a trivial solution to (6)-(8) is not admissible, and η_x and η_y remain constant because the states x and y do not appear in the Hamiltonian.) Moreover,

$$\begin{aligned} \min_{(u,v)\in\Omega} H(\eta_0^*,\vec{\eta}^{\,*},x^*,y^*,\psi^*,u,v) &= H(\eta_0^*,\vec{\eta}^{\,*},x^*,y^*,\psi^*,u^*,v^*) \\ &= 0 \end{aligned}$$

That is, the Hamiltonian is minimized with the optimal controls, and is equal to zero along the optimal trajectory, which is denoted by the superscript asterisk. (This notation is suppressed in the following for brevity.) Recalling that the adjoint variables η_x and η_y are constant, we may write

$$\eta_x = \eta\cos\theta \qquad \eta_y = \eta\sin\theta$$

for some constants η and θ. Then the differential equation for η_ψ can be rewritten as

$$\dot{\eta}_\psi = v\eta\sin(\psi-\theta) \tag{9}$$

and the variational Hamiltonian as

$$H = \eta_0\left(av^2+bv+c\right) + v\eta\cos(\theta-\psi) + \eta_\psi u \tag{10}$$

Characterizing the Extremal Controls

The Minimum Principle characterizes *extremal controls* as minimizers of the variational Hamiltonian. Here, we study the necessary conditions of the Minimum Principle to identify these extremal controls.

Lemma 1. *If $\eta_\psi \neq 0$ then $u = -\text{sgn}(\eta_\psi)u_{\max}$.*

Proof. Since the controls are not coupled in (10), then minimizing H with respect to u is equivalent to minimizing the term $\eta_\psi u$. Recall that $|u| \leq u_{\max}$. Thus the term $\eta_\psi u$ is minimized with $u = -\text{sgn}(\eta_\psi)u_{\max}$. The minimum value of $\eta_\psi u$ is then $-|\eta_\psi|u_{\max}$. Note that the minimum value of H is zero along an optimal trajectory (as required by the Minimum Principle). □

Lemma 2. *If η_ψ vanishes on an interval then $u = 0$ and $\psi = \theta$ or $\psi = \theta + \pi$.*

Proof. If η_ψ vanishes on an interval then $\dot{\eta}_\psi = 0$ for this interval. Given (9), consider the cases under which the condition $\dot{\eta}_\psi = 0$ holds:

1. $v = 0$, but $v \neq 0$ by assumption.
2. $\eta = 0$, then a necessary condition is that $H = \eta_0 w(v) = 0$. Since $w(v) > 0$ by assumption then $\eta_0 = 0$. However, the Minimum Principle does not allow a trivial solution to the adjoint equation.
3. $\sin(\psi-\theta) = 0$, and since θ is a constant, then $\psi = \theta$ or $\psi = \theta + \pi$ and $u = 0$.

Only the third case is admissible. If $\eta_\psi = 0$ at isolated points (rather than vanishing over a continuous interval), then these points correspond to discontinuities in the piecewise continuous control input and can be ignored. (Such points do not affect the solution.) □

Lemma 3. *($\mathcal{B}_{\text{stall}}$ extremals) If $\eta_0 = 0$, then $v = v_{\text{stall}}$, $u = -\text{sgn}(\eta_\psi)u_{\max}$, $\eta > 0$ and $\eta_\psi \neq 0$. Further, the change in heading along a $\mathcal{B}_{\text{stall}}$ extremal is $|\Delta\psi| < \pi$.*

Proof. If $\eta_0 = 0$ and $\eta = 0$ then a necessary condition is $H = \eta_\psi u = 0$. Considering Lemma 1 and Lemma 2, this requires $\eta_\psi = 0$. However, the Minimum Principle does not allow a trivial solution to the adjoint equation. Alternatively, if $\eta > 0$ then a necessary condition is

$$H = v\eta\cos(\theta-\psi) + \eta_\psi u = 0 \tag{11}$$

Since (11) is linear in v, the minimizing speed control may be on the boundary of the admissible speed interval $[v_{\text{stall}}, v_{\max}]$ depending on the sign of $\cos(\theta-\psi)$ (the slope of the linear Hamiltonian). Consider several cases under which (11) is minimized with respect to v:

1. if $\cos(\theta-\psi) > 0$, then the first term in (11) is strictly positive and, from Lemma 1, the second term $\eta_\psi u = -|\eta_\psi|u_{\max} \leq 0$. Then the necessary conditions are met if $v = v_{\text{stall}}$ minimizes the linear Hamiltonian and, from $H = 0$, we require

$$|\eta_\psi| = \frac{v_{\text{stall}}\eta\cos(\theta-\psi)}{u_{\max}} \tag{12}$$

2. if $\cos(\theta-\psi)=0$, then $\psi=\theta+\pi/2$ or $\psi=\theta+3\pi/2$ and H is independent of v. However, from (9) it is clear that at these headings $\dot{\eta}_\psi \neq 0$ and thus $\eta_\psi \neq 0$ (except at isolated points). This implies that $u \neq 0$, so that a constant heading cannot be maintained.

3. if $\cos(\theta-\psi)<0$, then it is clear that $H<0$ and the necessary condition $H=0$ cannot be satisfied.

Only the first case is admissible. The corresponding extremal path is a constant speed turn (left or right) with radius $v_{\text{stall}}/u_{\max}$. The change in heading is $|\Delta\psi|<\pi$ since $\cos(\theta-\psi)>0$ is required. We denote this extremal with the symbol $\mathcal{B}_{\text{stall}}$ to indicate that it is a "bang" (maximum) turn-rate control input at the stall speed. □

Lemma 4. *If $\eta_0>0$, then the critical point v_{crit} of H with respect to v is a minimum. Further, if $\eta>0$ then $v_{\text{crit}}=v_{\text{ms}}+\lambda\cos(\psi-\theta)$ where $\lambda=\eta/(2\eta_0 a)>0$. Otherwise, if $\eta=0$ then $v_{\text{crit}}=v_{\text{ms}}$.*

Proof. The condition for a critical point of H with respect to v is

$$\left.\frac{\partial H}{\partial v}\right|_{v=v_{\text{crit}}} = 2\eta_0 a v_{\text{crit}} + \eta_0 b + \eta\cos(\theta-\psi) = 0$$

and assuming $\eta_0>0$,

$$v_{\text{crit}} = \frac{-(\eta_0 b+\eta\cos(\theta-\psi))}{2\eta_0 a} \tag{13}$$

Since $\frac{\partial^2 H}{\partial v^2}=2\eta_0 a>0$, this critical point is a minimum. Substituting (13) into (10), a necessary condition is that

$$H=-\eta_0 a v_{\text{crit}}^2+\eta_0 c+\eta_\psi u=0 \tag{14}$$

With Assumption 2 the critical point (13) becomes

$$v_{\text{crit}}=v_{\text{ms}}-\lambda\cos(\psi-\theta) \tag{15}$$

Otherwise, if $\eta=0$ then (13) becomes

$$v_{\text{crit}}=\frac{-b}{2a}=v_{\text{ms}} \tag{16}$$

□

Lemma 5. *($\mathcal{B}_{\text{ms}}$ extremals) If $\eta_0>0$ and $\eta=0$, then $v=v_{\text{ms}}$, $u=-\text{sgn}(\eta_\psi)u_{\max}$ and $\eta_\psi\neq 0$.*

Proof. If $\eta=0$ then from (16) $v_{\text{crit}}=v_{\text{ms}}$ and, by Assumption 2, this is an admissible control that minimizes H. (It is clear that this is a global minimum since H is quadratic in v.) If $\eta_\psi=0$, then $H=\eta_0 w(v_{\text{ms}})>0$ so this case is not admissible. Alternatively, if $\eta_\psi\neq 0$ then a necessary condition is $H=\eta_0 w(v_{\text{ms}})-|\eta_\psi|u_{\max}=0$ which may be satisfied by a non-zero constant η_ψ. (Since $\eta=0$ then (9) implies that η_ψ is a constant and the turn rate is fixed.) The corresponding extremal path is a constant speed turn (left or right) with radius $v_{\text{ms}}/u_{\max}$. We denote this extremal with the symbol $\mathcal{B}_{\text{ms}}$ to indicate it corresponds to a bang turn-rate control input at minimum sink speed. □

Lemma 6. *($\mathcal{S}$ extremals) If $\eta_0>0$, $\eta>0$ and $\eta_\psi=0$, then $v=v_{\text{stf}}$, $u=0$, $\psi=\theta+\pi$ and $\lambda=v_{\text{stf}}-v_{\text{ms}}$.*

Proof. If $\eta_\psi=0$, then $u=0$ and (14) gives

$$v_{\text{crit}}=\pm\sqrt{\frac{c}{a}}=\pm v_{\text{stf}} \tag{17}$$

Only the positive case is admissible and the corresponding extremal trajectory is a straight line flown with speed v_{stf}. We denote this extremal with the symbol $\mathcal{S}$. This extremal control is analogous to MacCready's result [1] (in still air). From Lemma 4, v_{crit} is given in an alternative form by (15). Recall from Lemma 2 that $\eta_\psi=0$ occurs with $\psi=\theta$ or $\psi=\theta+\pi$ and from Assumption 3 $v_{\text{stf}}>v_{\text{ms}}$. Thus for (17) and (15) to be equivalent $\psi=\theta+\pi$ and $\lambda=v_{\text{stf}}-v_{\text{ms}}$. □

Lemma 7. *($\mathcal{B}$ extremals) If $\eta_0>0$, $\eta>0$ and $\eta_\psi\neq 0$, then $v=v_{\text{ms}}-\lambda\cos(\psi-\theta)$ and $u=-sgn(\eta_\psi)u_{\max}$.*

Proof. If $\eta_0>0$ and $\eta>0$, the critical point of H with respect to v is (15). If this critical point is in the admissible speed range $[v_{\text{stall}},v_{\max}]$, then it is the minimum of H. Otherwise, the minimum must occur on the boundary of the interval $[v_{\text{stall}},v_{\max}]$. With a fixed turn rate (9) becomes

$$\frac{d\eta_\psi}{d\psi}=\frac{d\eta_\psi}{dt}\left(\frac{d\psi}{dt}\right)^{-1}=\left(\frac{v\eta}{u}\right)\sin(\psi-\theta) \tag{18}$$

Suppose the extremal begins at time t_a with $\psi(t_a)=\psi_a$. Then for a fixed speed (e.g., v_{stall} or $v_{\max}$) and fixed turn rate we integrate (18) to obtain

$$\eta_\psi(\psi)-\eta_\psi(\psi_a)=\left(\frac{-v\eta}{u}\right)(\cos(\psi-\theta)-\cos(\psi_a-\theta)) \tag{19}$$

Substituting (19) into the Hamiltonian (10) gives

$$\begin{aligned} H &= \eta_0 w(v)+v\eta\cos(\theta-\psi) \\ &\quad -\left[\left(\frac{-v\eta}{u}\right)(\cos(\psi-\theta)-\cos(\psi_a-\theta))+\eta_\psi(\psi_a)\right]u \\ &= 2v\eta\cos(\theta-\psi)+\underbrace{\eta_0 w(v)-v\eta\cos(\psi_a-\theta)+\eta_\psi(\psi_a)u}_{\text{a constant}} \end{aligned} \tag{20}$$

Clearly, (20) cannot remain constant ($H=0$) with v and u fixed since ψ changes during a turn. It follows that if an extremal control exists, the corresponding speed control is given by the heading dependent speed (15) with the condition that $v_{\text{crit}}\in[v_{\text{stall}},v_{\max}]$. This extremal is denoted $\mathcal{B}$ to indicate a "bang" turn-rate control input. □

Theorem 1. *The set $\{\mathcal{B}_{\text{stall}},\mathcal{B}_{\text{ms}},\mathcal{S},\mathcal{B}\}$ contains all the extremal controls.*

Proof. In the preceding work, all admissible forms of the adjoint vector were considered. The results are summarized in Table 1, where explicit reference to adjoint components implies they are not identically zero, and time dependence of adjoint variables is indicated explicitly. □

Table 1: Candidate extremals

Symbol	Adjoint Vector	Speed & Turn Rate Control
$\mathcal{B}_{\text{stall}}$	$\begin{pmatrix} 0 \\ \eta \\ \eta_\psi(t) \end{pmatrix}$	$v = v_{\text{stall}}$ $u \in \{-u_{\max}, u_{\max}\}$
$\mathcal{B}_{\text{ms}}$	$\begin{pmatrix} \eta_0 \\ 0 \\ \eta_\psi \end{pmatrix}$	$v = v_{\text{ms}}$ $u \in \{-u_{\max}, u_{\max}\}$
$\mathcal{S}$	$\begin{pmatrix} \eta_0 \\ \eta \\ 0 \end{pmatrix}$	$v = v_{\text{stf}}$ $u = 0$
$\mathcal{B}$	$\begin{pmatrix} \eta_0 \\ \eta \\ \eta_\psi(t) \end{pmatrix}$	$v = v_{\text{ms}} - \lambda\cos(\psi - \theta)$ $u \in \{-u_{\max}, u_{\max}\}$

Additional Optimality Conditions

Having identified the set $\{\mathcal{B}_{\text{stall}}, \mathcal{B}_{\text{ms}}, \mathcal{S}, \mathcal{B}\}$ of all extremals, we consider the possible sequences in which these extremals can be joined. We refer to a sequence of extremal symbols (e.g., $\mathcal{BSB}$), read left to right, as a *word*. Since the adjoint variables η_0, η (equivalently, η_x and η_y) are constants, it is clear from Table 1 that only certain words can be formed. In this section, sub-optimality conditions are identified that restrict the optimal control to a finite and sufficient set of extremal sequences. To aid in this analysis, the paths corresponding to the extremal controls are parametrized in Appendix A.

Lemma 8. *Switches in the turn rate u only occur when* $\eta_\psi = 0$.

Proof. This follows immediately from Lemma 1 and Lemma 2, since switches between successive turns occur when η_ψ changes sign, and switches between turns and straight segments (or vice versa) occur with $\eta_\psi = 0$. □

Lemma 9. $\mathcal{B}_{\text{stall}}$ *extremal segments can only be joined to other* $\mathcal{B}_{\text{stall}}$ *extremal segments. Further, if a* $\mathcal{B}_{\text{stall}}$ *arc joins other* $\mathcal{B}_{\text{stall}}$ *arcs (of the opposite sense) on both ends, then it corresponds to a heading change* $|\Delta\psi| = \pi$

Proof. A $\mathcal{B}_{\text{stall}}$ extremal is the only extremal with $\eta_0 = 0$. Because η_0 remains constant, when η_ψ changes sign, the switch can only be to another $\mathcal{B}_{\text{stall}}$ extremal of the opposite sense. (As discussed in Lemma 3, $\eta_\psi \neq 0$ except at isolated points.) Since extremal switches occur only with $\eta_\psi = 0$, consider a $\mathcal{B}_{\text{stall}}$ extremal that begins at time t_a with heading ψ_a and ends at time t_b with heading ψ_b. If this $\mathcal{B}_{\text{stall}}$ extremal arc connects to other $\mathcal{B}_{\text{stall}}$ arcs at t_a and t_b, then it follows that $\eta_\psi(t_a) = \eta_\psi(t_b) = 0$. For a fixed speed $v = v_{\text{ms}}$, and fixed turn rate control u, setting the expression (19) to zero gives $\cos(\psi_b - \theta) = \cos(\psi_a - \theta) = 0$ which is satisfied with $\psi_a = \{\theta + \pi/2, \theta + 3\pi/2\}$ and either $\psi_b = \psi_a$ or $\psi_b = \psi_a + \pi$. The former case corresponds to a complete revolution so that the end state coincides with the initial state, and thus it is suboptimal. The latter case implies the heading change is $|\Delta\psi| = \pi$. □

Lemma 10. *An extremal control that contains a* $\mathcal{B}_{\text{stall}}$ *extremal segment is of the form* $\mathcal{B}_{\text{stall}}\mathcal{B}_{\text{stall}}\mathcal{B}_{\text{stall}}\mathcal{B}_{\text{stall}}$ *(or a subset thereof). If the sum of the angle magnitudes subtended by this extremal sequence is* $\geq 3\pi$*, then this sequence is suboptimal.*

Proof. From Lemma 3, $\mathcal{B}_{\text{stall}}$ segments are admissible only when $\cos(\theta - \psi) > 0$. In a sequence of $\mathcal{B}_{\text{stall}}$ arcs, the "middle" $\mathcal{B}_{\text{stall}}$ arc that joins to other $\mathcal{B}_{\text{stall}}$ arcs (of the opposite sense) must have a heading change $|\Delta\psi| = \pi$ (Lemma 9). Thus, in such a sequence, successive $\mathcal{B}_{\text{stall}}$ turns must occur at the isolated points where $\cos(\theta - \psi) = 0$, and so the heading is $\psi = \theta + \pi/2$ or $\psi = \theta + 3\pi/2$ at these isolated switching points.

Consider a series of $\mathcal{B}_{\text{stall}}$ extremals as shown in Fig. 3. At the points C, E, and G, the heading is either $\psi = \theta + \pi/2$ or $\psi = \theta + 3\pi/2$ corresponding to the switching points between successive $\mathcal{B}_{\text{stall}}$ arcs. The path between two such heading angles is a semicircular arc with $\psi = \theta$ at the midpoint of the arc (see points D and F). Further, any $\mathcal{B}_{\text{stall}}$ extremal subtending an angle $\geq \pi/2$ contains $\psi = \theta$ (see points B and H). It is clear that any sequence of $\mathcal{B}_{\text{stall}}$ arcs whose subtended (unsigned) angles sum to at least 3π will contain three points where the heading angle is $\psi = \theta$. The first and third occurrence of $\psi = \theta$ in such a sequence can be joined by a straight line segment (e.g. line DH or BF). This line segment can be flown with the same constant speed (and sink rate) as the $\mathcal{B}_{\text{stall}}$ arcs. Since the straight segment is shorter, it has a lower cost and it follows that the $\mathcal{B}_{\text{stall}}$ sequence is suboptimal. The longest sequence of $\mathcal{B}_{\text{stall}}$ arcs for which the sum of subtended (unsigned) angles is less than 3π is $\mathcal{B}_{\text{stall}}\mathcal{B}_{\text{stall}}\mathcal{B}_{\text{stall}}\mathcal{B}_{\text{stall}}$, with the condition that the initial and final arcs subtend angles with magnitude $< \pi/2$. □

Lemma 11. *A* $\mathcal{B}_{\text{ms}}$ *extremal cannot join other extremals, and has a heading change* $|\Delta\psi| < 2\pi$.

Proof. Along a $\mathcal{B}_{\text{ms}}$ arc the turn rate is $u = -\text{sgn}(\eta_\psi)u_{\max}$. From Lemma 5, η_ψ is a non-zero constant. Therefore the turn rate cannot change (Lemma 8) and other extremals cannot be joined to the $\mathcal{B}_{\text{ms}}$ arc. A $\mathcal{B}_{\text{ms}}$ arc with a heading change $|\Delta\psi| \geq 2\pi$ returns to the starting point, which is clearly suboptimal. □

Lemma 12. *An extremal control sequence containing* $\mathcal{B}$ *and* $\mathcal{S}$ *extremals, cannot join other types of extremals, and* λ *in* (15) *is* $\lambda = v_{\text{stf}} - v_{\text{ms}}$.

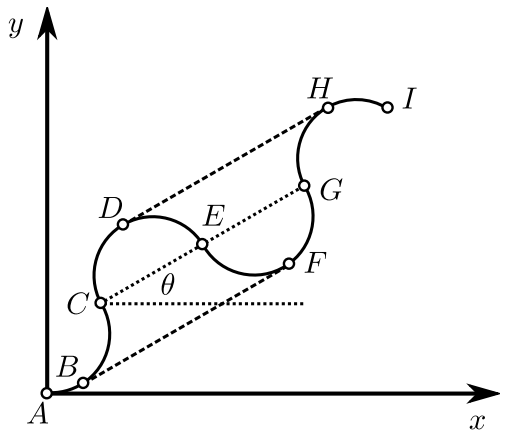

Fig. 3: A suboptimal $\mathcal{B}^{\text{stall}}\mathcal{B}^{\text{stall}}\mathcal{B}^{\text{stall}}\mathcal{B}^{\text{stall}}$ extremal sequence.

Proof. From Lemma 10 and Lemma 11, $\mathcal{B}$ and $\mathcal{S}$ extremals cannot join $\mathcal{B}_{\text{stall}}$ or $\mathcal{B}_{\text{ms}}$ extremals. For both $\mathcal{B}$ and $\mathcal{S}$ segments the conditions $\eta_0 > 0$ and $\eta \neq 0$ hold. When $\eta_\psi = 0$ a switch may occur between these two extremals. From Lemma 6, $\mathcal{S}$ segments require $\lambda = v_{\text{stf}} - v_{\text{ms}}$. Thus λ is a fixed in (15) for $\mathcal{B}$ arcs that join $\mathcal{S}$ segments. Further, this implies that the speed input along the $\mathcal{B}$ arc is $v \in [2v_{\text{ms}} - v_{\text{stf}}, v_{\text{stf}}]$, and by Assumption 4, this is an admissible control. □

Lemma 13. *If a $\mathcal{B}$ extremal contains a heading angle $\psi = \theta$, then $\lambda \leq v_{\text{ms}} - v_{\text{stall}}$.*

Proof. If a sequence of $\mathcal{B}$ arcs does not join a $\mathcal{S}$ segment, then Lemma 12 does not apply, and λ is a free parameter. The speed along a $\mathcal{B}$ extremal is given by $v = v_{\text{ms}} - \lambda\cos(\psi - \theta)$ where $v \in [v_{\text{stall}}, v_{\text{max}}]$. If $\psi = \theta$ the speed is at the minimum $v = v_{\text{ms}} - \lambda$. For this speed to be admissible $\lambda \leq v_{\text{ms}} - v_{\text{stall}}$ is required. □

Lemma 14. *If a $\mathcal{B}$ extremal contains two heading angles where $\psi = \theta + \pi$ then it is suboptimal.*

Proof. Consider a $\mathcal{B}$ extremal defined over the interval $[t_a, t_b]$ with $\psi(t_a) = \psi(t_b) = \theta + \pi$. The heading change is $|\Delta\psi| = 2\pi$ and, without loss of generality, it can be assumed that $x(t_a) = y(t_a) = 0$ and $\theta = \pi$ so that $\psi(t_a) = \psi(t_b) = 0$. Thus the vehicle begins at $\mathbf{x}_a = (0 \quad 0 \quad 0)^{\text{T}}$. Using (32)-(34), after one full revolution, the vehicle ends at $\mathbf{x}_b = (\pi\lambda/u_{\text{max}} \quad 0 \quad 0)^T$. Thus the states $\mathbf{x}_a$ and $\mathbf{x}_b$ can also be joined by a straight line segment of length $\pi\lambda/u_{\text{max}}$ with heading $\psi = 0$. Suppose this straight segment is flown with the same time-varying speed as the $\mathcal{B}$ extremal defined over the interval $[t_a, t_b]$. Since the straight segment is shorter, if it begins at $\mathbf{x}_a$ at time t_a it will reach $\mathbf{x}_b$ at a time $t_c < t_b$. Further, since the altitude is monotonically decreasing at the same rate along both paths, it follows that the straight segment will have a lower cost and that the $\mathcal{B}$ extremal is suboptimal. □

Corollary 1. *If an extremal control contains a $\mathcal{B}$ extremal segment, with no switching points and a heading change $|\Delta\psi| \geq 4\pi$, then it is suboptimal.*

Proof. If a $\mathcal{B}$ extremal arc subtends an angle $|\Delta\psi| \geq 4\pi$ and contains no switching points, then the turn rate is fixed and there exist two points t_a and t_b along the arc such that the heading $\psi(t_a) = \psi(t_b) = \theta$. Then by Lemma 14 this extremal is suboptimal. □

Lemma 15. *A $\mathcal{B}$ extremal that begins with heading ψ_a and ends with heading ψ_b, and for which η_ψ vanishes only at these boundary conditions, must contain the heading $\psi = (\psi_a + \psi_b)/2 = \theta$ and $\lambda \leq v_{\text{ms}} - v_{\text{stall}}$.*

Proof. With the change of variables $\phi = \psi - \theta$ the adjoint differential equation (9) becomes

$$\frac{d\eta_\psi}{d\phi} = \frac{d\eta_\psi}{dt}\left(\frac{d\phi}{dt}\right)^{-1} = \frac{\eta}{u}\underbrace{(v_{\text{ms}} - \lambda\cos\phi)}_{v(\phi)}\sin\phi \tag{21}$$

Consider a left turn ($u = u_{\text{max}}$) that begins with $\eta_\psi(t_a) = 0$ and $\phi(t_a) = \phi_a = \psi_a - \theta$, and ends with $\eta_\psi(t_b) = 0$ and $\phi(t_b) = \phi_b = \psi_b - \theta$. During this turn, ϕ (equivalently ψ) is increasing and $\eta_\psi < 0$. Let $\eta'_\psi(\phi)$ denote the value of $d\eta_\psi/d\phi$ as a function of ϕ, as given in (21). For η_ψ to become negative, the turn must begin at a point where $\eta'_\psi(\phi_a + \varepsilon) < 0$ for arbitrarily small ε. Since the speed $v(\phi)$ is always positive, then from (21) it is required that $\sin(\phi) < 0$ and therefore the turn must begin with $\phi_a \in [\pi, 2\pi)$. For all $\phi \in [\pi, 2\pi)$ the adjoint variable η_ψ is decreasing and at $\phi = 0$, η_ψ reaches a critical point corresponding to a minimum. Clearly the trajectory of η_ψ must contain this minimum point in order for η_ψ to then increase and vanish at ϕ_b. Since $\phi = 0$ implies $\psi = \theta$, then from Lemma 13 it follows that $\lambda \leq v_{\text{ms}} - v_{\text{stall}}$. Integrating (21) from ϕ_a to ϕ_b,

$$\eta_\psi(\phi_b) - \eta_\psi(\phi_a) = \frac{-\eta}{2u_{\text{max}}}(\cos\phi_a - \cos\phi_b)\,(-2v_{\text{ms}} + \lambda(\cos\phi_a + \cos\phi_b)) \tag{22}$$

If $\eta_\psi(\phi_a) = \eta_\psi(\phi_b) = 0$, then from (22) either

$$\frac{\cos\phi_a + \cos\phi_b}{2} = \frac{v_{\text{ms}}}{\lambda} \leq 1 \tag{23}$$

or

$$\cos\phi_a = \cos\phi_b \tag{24}$$

Since $\lambda \leq v_{\text{ms}} - v_{\text{stall}}$ and $v_{\text{stall}} > 0$ then $v_{\text{ms}}/\lambda > 1$ and the case (23) cannot hold. If (24) holds, then $\phi_b = \phi_a$ or $\phi_b = 2\pi - \phi_a$. The latter case occurs first as ϕ increases from ϕ_a. Further, it is clear that $\phi = 0$ is half way in between ϕ_a and ϕ_b. It follows that $\psi = (\psi_b + \psi_a)/2 = \theta$ is contained along the $\mathcal{B}$ extremal. Using similar arguments, it can be shown that these results also hold for right turns. □

Lemma 16. *If an extremal control contains $\mathcal{B}$ and $\mathcal{S}$ segments, then it is of the form $\mathcal{BSB}$ (or a subset thereof).*

Proof. Recall that all $\mathcal{S}$ segments have $\psi = \theta + \pi$. Thus if a $\mathcal{S}$ segment connects to a $\mathcal{B}$ arc at a point t_a then $\eta_\psi(t_a) = 0$ and $\psi(t_a) = \theta + \pi$. If this $\mathcal{B}$ arc is to join another extremal at time t_b then $\eta_\psi(t_b) = 0$. From Lemma 15 with $\psi(t_a) = \theta + \pi$ it follows that $\psi(t_b) = \theta - \pi = \psi(t_a)$, corresponding to a 2π change in heading. From Lemma 14 this $\mathcal{B}$ arc is suboptimal because it contains two points at which $\psi = \theta + \pi$. Thus a $\mathcal{SB}$ segment cannot be followed by another extremal. A similar argument can be made that $\mathcal{BS}$ segments cannot be preceeded by another extremal. Therefore all extremals containing $\mathcal{B}$ and $\mathcal{S}$ arcs must be of the form $\mathcal{BSB}$ (or a subset thereof). □

Lemma 17. *Consecutive $\mathcal{B}$ extremals, each beginning and ending with $\eta_\psi = 0$, are antisymmetric.*

Proof. From Lemma 15, the heading along a $\mathcal{B}$ extremal, beginning and ending with $\eta_\psi = 0$, goes from ψ_a to ψ_b. If this extremal arc is followed by a change in turn rate to another $\mathcal{B}$ extremal arc, the heading will go from ψ_b to ψ_a along this second arc. Further, since the speed is heading dependent, the extremal path followed by the second arc will be antisymmetric to that of the first. □

Lemma 18. *A sequence of three $\mathcal{B}$ arcs, that begin and end with $\eta_\psi = 0$, is suboptimal.*

Proof. Consider a sequence of three consecutive $\mathcal{B}$ arcs that each begin and end with $\eta_\psi = 0$. The corresponding extremal path is sketched in Fig. 4 where the extremal sequence begins at point A and ends at point F. Without loss of generality, assume that the initial $\mathcal{B}$ extremal arc transfers the vehicle from $\mathbf{x}_A = (0 \quad 0 \quad \psi_a)^{\mathrm{T}}$ to $\mathbf{x}_C = (\Delta x \quad \Delta y \quad \psi_c)^{\mathrm{T}}$. From Lemma 17 the second arc is anti-symmetric to the first and transfers the vehicle to $\mathbf{x}_D = (2\Delta x \quad 2\Delta y \quad \psi_a)^{\mathrm{T}}$. Similarly, the third arc transfers the vehicle to $\mathbf{x}_F = (3\Delta x \quad 3\Delta y \quad \psi_c)^{\mathrm{T}}$. It is clear that there will exist two points (e.g. B and E in Fig. 4), on the initial and final arc respectively, that can be connected via a straight line segment with heading

$$\varphi = \operatorname{atan}\left(\frac{\Delta y}{\Delta x}\right) \tag{25}$$

Suppose the straight segment is traversed with the same speed control as the $\mathcal{B}$ arcs from point B to E. Since the straight line path is shorter and the altitude is monotonically decreasing at the same rate for both paths, it will result in a lower cost. Thus the $\mathcal{BBB}$ sequence is suboptimal. □

Lemma 19. *Extremal controls containing only $\mathcal{B}$ arcs are of the form $\mathcal{BBBB}$ (or a subset thereof).*

Proof. In a sequence of $\mathcal{B}$ arcs, the $\mathcal{B}$ arcs that connect to other $\mathcal{B}$ arcs at both ends (i.e., the interior $\mathcal{B}$ arcs in $\mathcal{BBBB}$) are required to begin and end with $\eta_\psi = 0$. Thus they satisfy the conditions of Lemma 17 and Lemma 18. However the initial and final $\mathcal{B}$ arcs that join a boundary condition (i.e. the first and last $\mathcal{B}$ arcs in $\mathcal{BBBB}$) do not necessarily satisfy these same properties. (These $\mathcal{B}$ arcs may be truncated to satisfy the boundary conditions.) Thus the longest sequence of $\mathcal{B}$ extremals, in terms of the number of extremals, is of the form $\mathcal{BBBB}$ with the restriction that the initial and final $\mathcal{B}$ arcs are sufficiently short, such that they do not contain heading angles $\psi = \varphi$, given in (25). The same restriction applies to a $\mathcal{BBB}$ extremal sequence. Such sequences also require that the constant $\lambda \leq v_{\mathrm{ms}} - v_{\mathrm{stall}}$ by Lemma 15.

If the extremal sequence is of the form $\mathcal{BB}$ or $\mathcal{B}$ then Lemma 17 and Lemma 18 do not apply. In this case λ is restricted such that for all the heading angles traversed $v = v_{\mathrm{ms}} - \lambda\cos(\psi - \theta) \in [v_{\mathrm{stall}}, v_{\mathrm{max}}]$. A $\mathcal{BB}$ sequence will contain at least one point where $\eta_\psi = 0$ (corresponding to the switching point), whereas a $\mathcal{B}$ arc is not required to contain the point $\eta_\psi = 0$.

For brevity, we use the word $\mathcal{BBBB}$ to denote all of these extremal sequences (including those of the form $\mathcal{BBB}$, $\mathcal{BB}$, and $\mathcal{B}$), recognizing that for each sequence there are unique constraints on the extremal arcs. □

Theorem 2. *The set*

$$\Gamma = \{\mathcal{BSB},\ \mathcal{BBBB},\ \mathcal{B}_{\mathrm{ms}},\ \mathcal{B}_{\mathrm{stall}}\mathcal{B}_{\mathrm{stall}}\mathcal{B}_{\mathrm{stall}}\mathcal{B}_{\mathrm{stall}}\} \tag{26}$$

of extremal controls contains the optimal control.

Proof. In Theorem 1 it was shown that the set $\{\mathcal{B}_{\mathrm{stall}}, \mathcal{B}_{\mathrm{ms}}, \mathcal{S}, \mathcal{B}\}$ contains all candidate extremals. In Lemma 10 it was shown that all extremal controls containing $\mathcal{B}_{\mathrm{stall}}$ arcs are of the form $\mathcal{B}_{\mathrm{stall}}\mathcal{B}_{\mathrm{stall}}\mathcal{B}_{\mathrm{stall}}\mathcal{B}_{\mathrm{stall}}$ (or a subset thereof). In Lemma 11 it was shown that $\mathcal{B}_{\mathrm{ms}}$ extremals cannot join other extremals. In Lemma 16 it was shown that if an extremal control contains $\mathcal{B}$

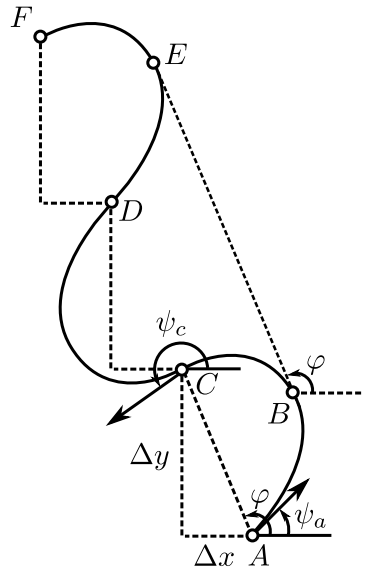

Fig. 4: The sequence of three $\mathcal{B}$ extremal arcs, that each begin and end with $\eta_\psi = 0$, is suboptimal.

and $\mathcal{S}$ segments, then it is of the form $\mathcal{BSB}$ (or a subset thereof). Last, in Lemma 19, it was shown that extremal controls containing only $\mathcal{B}$ arcs are of the form $\mathcal{BBBB}$ (or a subset thereof). Thus it follows that Γ is a finite and sufficient set of candidate extremal controls. It has been established that an optimal control exists, and therefore Γ contains the optimal control. □

Path Synthesis

The set Γ contains all of the extremal control sequences that are candidates for an optimal control. We refer to each member of Γ as a *class* of candidate controls. In Appendix A individual extremals are parametrized to describe their resulting planar displacements and heading changes. Similarly, each class of controls in Γ can be parametrized to give the glider's final state resulting from the corresponding extremal sequence. We denote the space of parameters admissible for a given class and path type as P. The *path synthesis* problem is to determine the specific optimal control history $\mathbf{u}^*(\cdot)$ (equivalently, the class in Γ and parameter $p \in P$) that minimizes the cost while satisfying the boundary conditions.

For a given class, solutions satisfying the boundary conditions may exist at several isolated points or neighborhoods in the parameter space. If the solutions exist at several isolated points, path synthesis is similar to a root finding problem. If there exist continuously parametrized sets of solutions, we seek to find the lowest cost (locally) optimal solution within each such neighborhood. Intuitively, we might expect that these locally optimal controls correspond to paths that are qualitatively distinct. (Paths within a class may be qualitatively distinct, for example, if the orientation or a number of extremals they contain is unique.)

Consider the class of $\mathcal{BSB}$ candidate optimal controls. If we denote left turns with the symbol L, right turns with R, and straight segments with S, then the set $\{LSL, LSR, RSL, RSR\}$ contains all the possible orientations of a $\mathcal{BSB}$ control. In this case, we might expect that the boundary conditions can be satisfied by several paths corresponding to different orientations. (For example, if the final endpoint is on the negative x-axis with heading $\psi = \pi$ then, by symmetry, any path to the endpoint can be reflected about the x-axis to obtain a path with the same cost but with a different orientation.) Similarly, controls in the class $\mathcal{BBBB}$, $\mathcal{B}_{\text{ms}}$ or $\mathcal{B}_{\text{stall}}\mathcal{B}_{\text{stall}}\mathcal{B}_{\text{stall}}\mathcal{B}_{\text{stall}}$ may either begin with a right (R) or left (L) turn and successive turns are of the opposite sense. Therefore there are two orientations to consider in these cases. If a particular extremal within a class has zero length then the corresponding control is unique in terms of the number (and sequence) of extremals. For example, if the $\mathcal{BSB}$ sequence contains one or more extremals of zero length, the controls may be of the form $\mathcal{BS}$, $\mathcal{SB}$, $\mathcal{BB}$, $\mathcal{B}$ or $\mathcal{S}$.

One approach to solving the path synthesis problem is to enumerate all of the locally optimal controls within each class, for all classes in Γ, and compare their respective costs. A numerical optimization routine that enumerates *all* locally optimal solutions would always give the globally optimal control (accurate to within a user specified tolerance). In practice however, it is difficult to construct such an algorithm. One may therefore expect only locally optimal paths, in general. In the Appendix we detail a method for computing the candidate controls for each class in Γ. We find that $\mathcal{BSB}$ controls can be easily computed by solving a root finding problem in one parameter, as shown in Appendix B. The class of $\mathcal{BBBB}$ paths is parametrized with more unknown variables than constraints and a unique solution is not available. Thus, in Appendix C, a constrained optimization problem is formulated to solve for the parameter vector p in this case. Last, in Appendix D it is shown that the parameters of $\mathcal{B}_{\text{ms}}$ or $\mathcal{B}_{\text{stall}}\mathcal{B}_{\text{stall}}\mathcal{B}_{\text{stall}}\mathcal{B}_{\text{stall}}$ extremals can be found algebraically (when they exist).

Illustrative Examples

To illustrate the path synthesis procedure, we assume a glider model that is representative of the DG-1001M motorglider. (This is a modern optionally powered glider, with a 20 meter wingspan, manufactured by DG Flugzeugbau in Germany.) The glide polar curve given in the DG-1001M flight manual [39], corresponding to a wing loading of 35 kg/m^2, was digitized and is indicated by the dashed line in Fig. 5. A quadratic curve was fit to this data to give an approximate glide polar (solid line in Fig. 5) expressed by the function:

$$w(v) = \underbrace{0.0002093}_{a} v^2 \underbrace{-0.0381}_{b} v + \underbrace{2.3146}_{c} \qquad (27)$$

where the units of sink rate w are in meters/second and the units of speed v are in kph (kilometers/hour). Since the previous analysis showed that the extremal controls are confined to the speed interval $v \in [v_{\text{stall}}, v_{\text{stf}}]$, only a subset of the available data was used for curve fitting. A data set was chosen that resulted in the smallest error between the approximate and actual stall, minimum sink and best glide flight conditions. Since flying at the

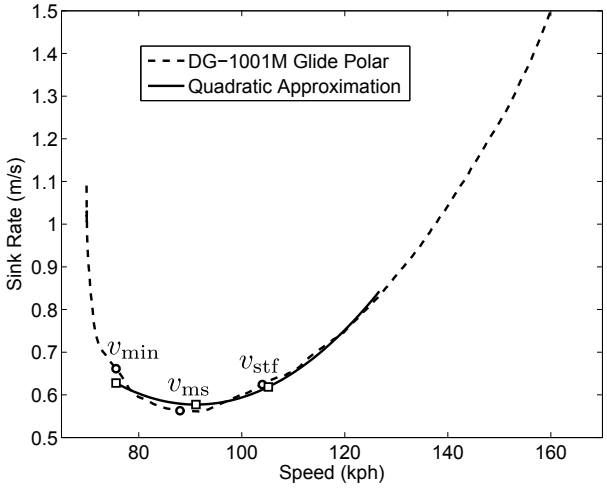

Fig. 5: Digitized glide polar of the DG-1001M motorglider (dashed line), adapted from [39], compared to a quadratic approximation (solid line).

stall speed is not desirable, and since this stall region deviates significantly from the parabolic shape of the remaining glide polar, the stall speed was artificially increased to $v_{\text{stall}} = 75.6$ kph. This is a more realistic minimum operating speed, and the quadratic glide polar is a better approximation of the data with this conservative assumption. The speed and sink rates at these various flight conditions are indicated with circle markers for actual values and square markers for approximate values in Fig. 5. The corresponding numeric values for these flight conditions are given in Table 2. With this tabulated data we may verify that Assumption 4 is satisfied by the quadratic approximation. (It is also satisfied by the actual glide polar if we use the actual stall speed.)

As discussed in Remark 1, we assume the glide polar $w(v)$ is independent of the turn rate u. This approximation is only valid for mild turns with very shallow bank angles. For the DG-1001M we assume the turn rate limit is $u_{\max} = \pi/15$ (radians/sec) (i.e., it takes 15 seconds to complete a turn with a 180 degree heading change). For the kinematic car model the minimum turn radius R scales with the speed: $R = v/u_{\max}$. Thus the approximate minimum turn radius at the speed to fly is about $R_{\text{stf}} = 139$ m, and at the stall speed the radius is about $R_{\text{stall}} = 100$ m. Note that the change in sink rate on the interval $[v_{\min}, v_{\text{stf}}]$ is very small compared to the changes in speed and turn radius. Over large distances a small change in sink rate may become significant, however on the scale of a few hundred meters these effects are not as pronounced. Instead, the altitude loss is largely influenced by the transit time to the goal. Intuitively, we might think that strictly operating at the speed to fly will minimize the altitude loss to the goal. However, the advantage of slowing down is that the minimum turning radius decreases, potentially allowing a shorter and faster path to the goal; with a smaller turn radius the reduction in transit time may be large enough to justify the penalty incurred by a small increase in sink rate. To demonstrate the path synthesis algorithm we select three final endpoints, plot the resulting candidate paths, and compare their costs (see Fig. 6a,7a and 8a). In each case the glider begins at the origin, pointed east along the x axis with $\mathbf{x}_0 = (0 \quad 0 \quad 0)^{\text{T}}$ and the candidate paths to the endpoint $\mathbf{x}_1$ are labeled with their path type, orientation, and cost. (The cost is altitude loss in meters and is given in square brackets next to each path.) For comparison, the Dubins path at the speed to fly is plotted in each case with a dashed line. Note that the x and y axes have been normalized by the turn radius at the speed to fly R_{stf}. Further, the optimal control history corresponding to the lowest cost path in each case is given in the adjacent plots (see Fig. 6b,7b and 8b). The turn rate limits and the speed limits at v_{stall} and v_{stf} are plotted with dashed lines.

Table 2: Comparison of approximate and actual speeds and sink rates at various flight conditions.

Flight Condition	Actual Speed (kph)	Approx. Speed (kph)	Actual Sink Rate (m/s)	Approx. Sink Rate (m/s)
Stall Speed	75.6	75.6	0.66	0.63
Minimum Sink	88.0	91.1	0.56	0.58
Speed to Fly	104.0	105.2	0.62	0.62

In Fig. 6 we have $\mathbf{x}_1 = (0 \quad R_{\text{stf}} \quad 2\pi/3)^{\text{T}}$ and the lowest cost control is of the type $\mathcal{BBB}$, with orientation *RLR*. Since this endpoint is very close to the initial state, significant maneuvering is required. In comparison to the Dubins path the altitude loss

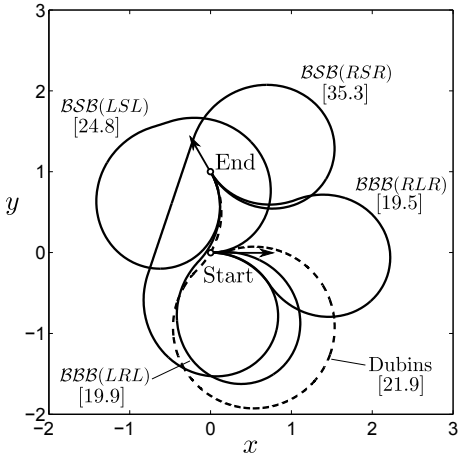

(a) Candidate paths

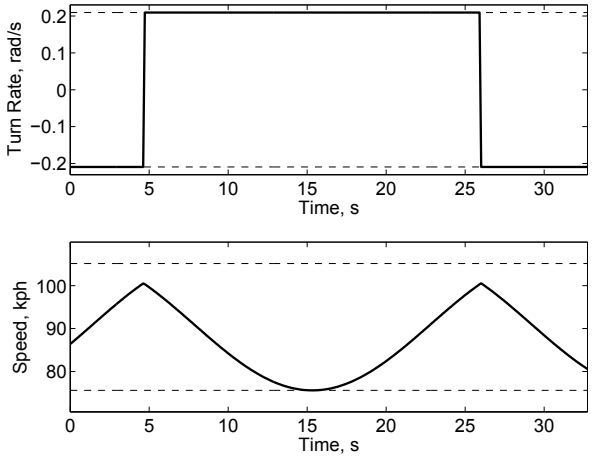

(b) Optimal control history

Fig. 6: Path synthesis result for the final state $\mathbf{x}_1 = (0 \quad R_{\text{stf}} \quad 2\pi/3)^{\text{T}}$. Change in altitude is indicated by square brackets.

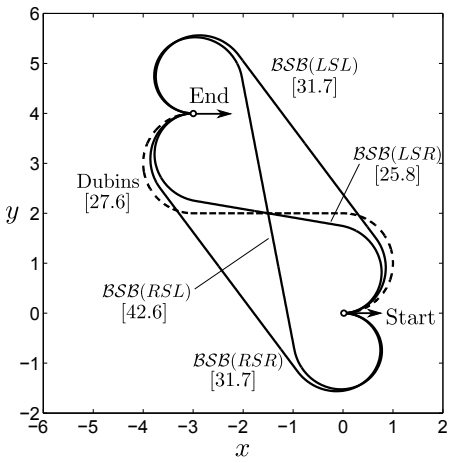

(a) Candidate paths

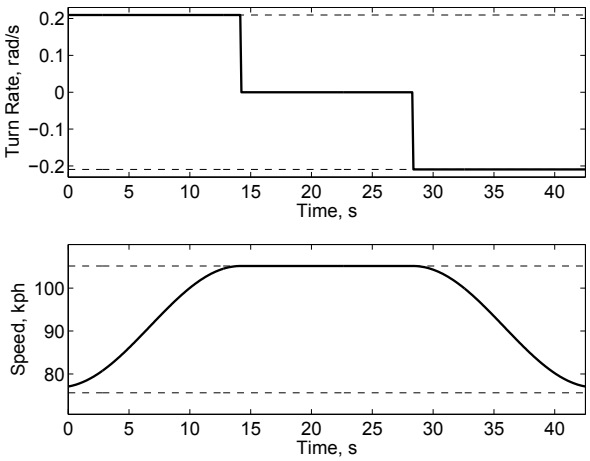

(b) Optimal control history

Fig. 7: Path synthesis result for the final state $\mathbf{x}_1 = (-3R_{\text{stf}} \quad 4R_{\text{stf}} \quad 0)^{\text{T}}$. Change in altitude is indicated by square brackets.

is reduced by 2.4 meters which is an 11% improvement. From the optimal control history in Fig. 6b, we find that the glider speed changes drastically and reaches the minimum speed (and smallest turn radius) in the middle of the second turn.

In Fig. 7 we have $\mathbf{x}_1 = (-3R_{\text{stf}} \quad 4R_{\text{stf}} \quad 0)^{\text{T}}$ and the lowest cost control is of the type $\mathcal{BSB}$, with orientation *LSR*. Since the endpoint is relatively far from the starting point, it cannot be reached by a $\mathcal{BBBB}$ candidate control. For endpoints that are sufficiently far away, we do not have to compute all candidate controls in Γ and instead may only check the $\mathcal{BSB}$ class of controls. In this case, the altitude loss is reduced by about 1.8 m or 6.5% relative to the Dubins path. Note the smooth transition in the speed control between the $\mathcal{B}$ and $\mathcal{S}$ extremals as shown in Fig. 7b.

Last, in Fig. 8 we have $\mathbf{x}_1 = (0 \quad 2R_{\text{stf}} \quad 7\pi/4)^{\text{T}}$ and the lowest cost control is of the type $\mathcal{BSB}$, with orientation *LSL*. It is interesting to note that the orientation of the Dubins path is also *LSL*. In this case the altitude loss is reduced by about 1.7 m or 7.8% relative to the Dubins path.

Conclusion

In this paper we consider the problem of minimizing altitude loss for a sailplane maneuvering in still air to a nearby position and heading angle. The sailplane is modeled as a kinematic car, with speed and turn rate controls, and with a sink rate that is a quadratic function of the speed. We find that the extremal controls correspond to straight segments flown at the best glide speed (denoted as $\mathcal{S}$ extremals) and maximum rate turns with either: a heading dependent speed in-

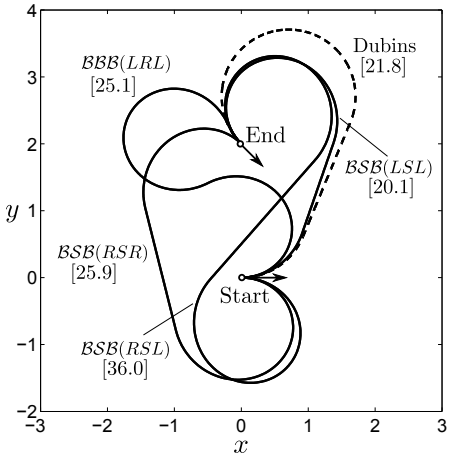

(a) Candidate paths

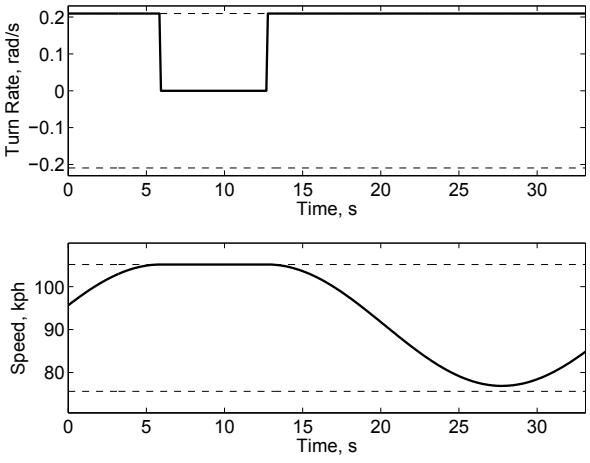

(b) Optimal control history

Fig. 8: Path synthesis result for the final state $\mathbf{x}_1 = (0 \quad 2R_{\text{stf}} \quad 7\pi/4)^{\text{T}}$. Change in altitude is indicated by square brackets.

put ($\mathcal{B}$ extremals), the stall speed ($\mathcal{B}_{\text{stall}}$ extremals), or the minimum sink speed ($\mathcal{B}_{\text{ms}}$ extremals). The optimal control is found to be a member of the finite and sufficient set $\Gamma = \{\mathcal{BSB},\ \mathcal{BBBB},\ \mathcal{B}_{\text{stall}}\mathcal{B}_{\text{stall}}\mathcal{B}_{\text{stall}}\mathcal{B}_{\text{stall}},\ \mathcal{B}_{\text{ms}}\}$. A path synthesis procedure is proposed to numerically solve for each candidate path in Γ, and to identify the lowest cost (locally) optimal control. An illustrative example, based on the DG-1001M motorglider, demonstrates a significant improvement in altitude loss resulting from the proposed approach when compared to a standard Dubins path planning algorithm (with a fixed speed for best level glide). One limitation of the proposed approach, however, is that we have assumed that sink rate does not vary with turn rate. The proposed algorithm is therefore appropriate for shallow banked turns where the sink rate remains relatively constant and for autonomous sailplanes that can track the required velocity and turn rate controls.

Acknowledgments

The authors gratefully acknowledge the support of the Office of Naval Research under Grant #N00014-13-1-0060.

References

[1] MacCready, P. B., "Optimum airspeed selector," *Soaring*, 1954, pp. 8–9.

[2] Stojkovic, B., "Generalized speed-to-fly theory," *Technical Soaring*, Vol. 17, No. 3, 1991, pp. 77–83.

[3] Pierson, B. L. and de Jong, J. L., "Cross-country sailplane flight as a dynamic optimization problem," *International Journal for Numerical Methods in Engineering*, Vol. 12, No. 11, 1978, pp. 1743–1759.

[4] de Oliveira, P. H. I. A. and de Freitas Pinto, R. L. U., "Flight path optimization for competition sailplanes through state variables parametrization," *18th International Congress of Mechanical Engineering*, 2005.

[5] Arho, R., "Some notes on soaring flight optimization theory," *OSTIV Publication XIV*, OSTIV, 1976.

[6] Dickmans, E. D., "Optimal dolphin-style soaring," *OSTIV Publication XVI*, OSTIV, 1981.

[7] Metzger, D. E. and Hedrick, J. K., "Optimal flight paths for soaring flight," *Journal of Aircraft*, Vol. 12, No. 11, 1975, pp. 867–871.

[8] Cochrane, J. H., "MacCready theory with uncertain lift and limited altitude," *Technical Soaring*, Vol. 23, No. 3, 1999, pp. 88–96.

[9] Kolmanovsky, I. V. and Menezes, A. A., "A stochastic drift counteraction optimal control approach to glider flight management," *American Control Conference*, IEEE, 2011.

[10] Almgren, R. and Tourin, A., "Optimal soaring via Hamilton-Jacobi-Bellman equations," *Optimal Control Applications and Methods*, Vol. 36, No. 4, 2015, pp. 475–495.

[11] Chakrabarty, A. and Langelaan, J. W., "Energy-based long-range path planning for soaring-capable unmanned aerial vehicles," *Journal of Guidance, Control, and Dynamics*, Vol. 34, No. 4, 2011, pp. 1002–1015.

[12] Federal Aviation Administration, "Accident prevention program: impossible turn," Tech. Rep. FAA-P-8740-44, Washington, D.C., 1987.

[13] Rogers, D. F., "Possible "impossible" turn," *Journal of Aircraft*, Vol. 32, No. 2, 1995, pp. 392–397.

[14] Hoffren, J. and Raivio, T., "Optimal maneuvering after engine failure," *AIAA Atmospheric Flight Mechanics Conference*, AIAA, 2000.

[15] Brinkman, K. and Visser, H. G., "Optimal turn-back manoeuvre after engine failure in a single-engine aircraft during climb-out," *Proceedings of the Institution of Mechanical Engineers, Part G: Journal of Aerospace Engineering*, Vol. 221, No. G, 2007, pp. 17–27.

[16] Adler, A., Bar-Gill, A., and Shimkin, N., "Optimal flight paths for engine-out emergency landing," *24th Chinese Control and Decision Conference*, IEEE, 2012.

[17] Dubins, L. E., "On curves of minimal length with a constraint on average curvature, and with prescribed initial and terminal positions and tangents," *American Journal of Mathematics*, Vol. 79, No. 3, 1957, pp. 497–516.

[18] Atkins, E. M., Portillo, I. A., and Strube, M. J., "Emergency flight planning applied to total loss of thrust," *Journal of Aircraft*, Vol. 43, No. 4, 2006, pp. 1205–1216.

[19] Eng, P., Mejias, L., Walker, R., and Fitzgerald, D., "Guided chaos: path planning and control for a UAV-forced landing," *IEEE Robotics & Automation Magazine*, Vol. 17, No. 2, 2010, pp. 90–98.

[20] Yomchinda, T., Horn, J. F., and Langelaan, J. W., "Modified Dubins parameterization for aircraft emergency trajectory planning," *Proceedings of the Institution of Mechanical Engineers, Part G: Journal of Aerospace Engineering. (DOI: 10.1177/0954410016638869)*, 2016.

[21] Chitsaz, H. and LaValle, S. M., "Time-optimal paths for a Dubins airplane," *46th IEEE Conference on Decision and Control*, IEEE, 2007.

[22] Djath, K., Siadet, A., Dufaut, M., and Wolf, D., "Navigation of a mobile robot by locally optimal trajectories," *Robotica*, Vol. 17, No. 5, 1999, pp. 553–562.

[23] Mahmoudian, N., Geisbert, J., and Woolsey, C. A., "Approximate analytical turning conditions for underwater gliders: implications for motion control and path planning," *IEEE Journal of Oceanic Engineering*, Vol. 35, No. 1, 2010, pp. 131–143.

[24] Techy, L. and Woolsey, C. A., "Minimum-time path planning for unmanned aerial vehicles in steady uniform winds," *Journal of Guidance, Control, and Dynamics*, Vol. 32, No. 6, 2009, pp. 1736–1746.

[25] Maggiar, A. and Dolinskaya, I. S., "Construction of fastest curvature-constrained paths in direction-dependent media," *Journal of Guidance, Control, and Dynamics*, Vol. 37, No. 3, 2014, pp. 813–827.

[26] Wolek, A. and Woolsey, C., "Feasible Dubins paths in presence of unknown, unsteady velocity disturbances," *Journal of Guidance, Control, and Dynamics*, Vol. 38, No. 4, 2015, pp. 782–787.

[27] Choi, H. and Atkins, E. M., "Smooth transitions for a turning Dubins vehicle," *AIAA Guidance, Navigation, and Control Conference*, AIAA, 2010.

[28] Bakolas, E. and Tsiotras, P., "Optimal synthesis of the asymmetric sinistral/dextral Markov-Dubins problem," *Journal of Optimization Theory and Applications*, Vol. 150, No. 2, 2011, pp. 233–250.

[29] Williamson, W. E., "Minimum and maximum endurance trajectories for gliding flight in a horizontal plane," *Journal of Guidance, Control, and Dynamics*, Vol. 2, No. 6, 1979, pp. 457–462.

[30] Chern, J.-S., "Isochrones for maximum endurance horizontal gliding flight," *Journal of Guidance, Control, and Dynamics*, Vol. 8, No. 1, 1984, pp. 148–150.

[31] Finke, K., "Comparison of classical speed to fly theory using second, third, fourth and fifth degree polynomial speed polars," *Technical Soaring*, Vol. 16, No. 3, 1992, pp. 78–76.

[32] Danewid, R., "A simple approximation of the best-speed-to-fly theory," *Technical Soaring*, Vol. 12, No. 3, 1988, pp. 83–88.

[33] Milgram, J., "Climb performance and handicapping," *Skylines*, Skyline Soaring Club, Front Royal, VA, 2005.

[34] Coombes, M., Chen, W.-H., and Render, P., "Reachability analysis of landing sites for forced landing of a UAS," *International Conference on Unmanned Aircraft Systems*, IEEE, 2013.

[35] Steinberg, A. M. and Stalford, H. L., "On existence of optimal controls," *Journal of Optimization Theory and Applications*, Vol. 11, No. 3, 1973, pp. 266–273.

[36] Lee, E. B. and Markus, L., "Necessary and sufficient conditions for optimal control," *Foundations of Optimal Control Theory*, John Wiley & Sons, 1967, pp. 308–363.

[37] Leitmann, G., "Regular optimal trajectories," *The Calculus of Variations and Optimal Control*, Plenum Press, 1981, pp. 99–124.

[38] Pontryagin, L. S., Boltyanskii, V. G., Gamkrelidze, R. V., and Mischcenko, E. F., *The mathematical theory of optimal processes*, Interscience Publishers, 1962.

[39] DG Flugzeugbau Gmbh, "Flight manual for the motorglider DG-1001M," Tech. Rep. EASA.A.072, Bruchsal, Germany, 2010.

[40] Chebfun, *ver. 4.2*, Oxford University Mathematical Institute, Oxford, England, 2013.

[41] MATLAB, *ver. 8.2.0*, The MathWorks, Inc., 2013.

Appendix

A Parameterizing the Extremal Controls

The extremal controls are given in Table 1. If the glider employs a given extremal control for some duration, the result will be a change in the state (heading and position) and cost (altitude). To aid in further analysis, we may uniquely parametrize extremal controls to quantify such changes. Recall that an $\mathcal{S}$ extremal has speed $v = v_{\text{stf}}$ and turn rate $u = 0$. This straight line path can be parametrized by its length L and initial heading angle ψ_i. In this case, the state and cost rates are fixed, and the time to traverse the length L is simply L/v_{stf}. Thus the changes in heading ($\Delta\psi_{\mathcal{S}}$), planar positions ($\Delta x_{\mathcal{S}}$ and $\Delta y_{\mathcal{S}}$), and altitude $\Delta h_{\mathcal{S}}$, are obtained by multiplying the fixed state and cost rates by the time interval L/v_{stf}:

$$\Delta\psi_{\mathcal{S}}(L,\psi_i) = 0 \tag{28}$$

$$\Delta x_{\mathcal{S}}(L,\psi_i) = L\cos\psi_i \tag{29}$$

$$\Delta y_{\mathcal{S}}(L,\psi_i) = L\sin\psi_i \tag{30}$$

$$\Delta h_{\mathcal{S}}(L,\psi_i) = L\left(av_{\text{stf}} + b + \frac{c}{v_{\text{stf}}}\right) \tag{31}$$

$\mathcal{B}$ extremal arcs have $v = v_{\text{ms}} - \lambda\cos(\psi-\theta)$ and $|u| = u_{\max}$ and can be parametrized by the initial heading ψ_i, the change in heading δ, and the parameters θ and λ. These extremals correspond to a fixed turn rate and we may change the independent variable from t to ψ where $dt = (\text{sgn}(\delta)/u_{\max})d\psi$. Then integrating the equations of motion (1)-(3) and the cost functional (4) with respect to ψ, we obtain the changes in state and cost:

$$\Delta\psi_{\mathcal{B}}(\psi_i,\delta,\theta,\lambda) = \delta \tag{32}$$

$$\Delta x_{\mathcal{B}}(\psi_i,\delta,\theta,\lambda) = \text{sgn}(\delta)\left(\frac{v_{\text{ms}}[\sin(\psi_i+\delta)-\sin\psi_i] - \frac{1}{2}\lambda[\delta\cos\theta + \cos(2\psi_i-\theta+\delta)\sin\delta]}{u_{\max}}\right) \tag{33}$$

$$\Delta y_{\mathcal{B}}(\psi_i,\delta,\theta,\lambda) = \text{sgn}(\delta)\left(\frac{v_{\text{ms}}[\cos\psi_i-\cos(\psi_i+\delta)] - \frac{1}{2}\lambda[\delta\sin\theta + \sin(2\psi_i-\theta+\delta)\sin\delta]}{u_{\max}}\right) \tag{34}$$

$$\Delta h_{\mathcal{B}}(\psi_i,\delta,\theta,\lambda) = \left(\frac{\text{sgn}(\delta)}{u_{\max}}\right)\left[(av_{\text{ms}}^2 + bv_{\text{ms}} + c + \frac{1}{2}a\lambda^2)\delta + \frac{a\lambda^2}{2}\sin\delta\cos(\delta+2\psi_i-2\theta) - 2\lambda(b+2av_{\text{ms}})\cos\left(\frac{\delta}{2}+\psi_i-\theta\right)\sin\left(\frac{\delta}{2}\right)\right] \tag{35}$$

Likewise, $\mathcal{B}_{\text{stall}}$ (or $\mathcal{B}_{\text{ms}}$) extremal arcs have $|u| = u_{\max}$ and $v = v_{\text{stall}}$ (or $v = v_{\text{ms}}$). Such extremals can be parametrized by the initial orientation ψ_i, and the change in heading δ. Choosing v appropriately, the changes in state and cost, for both $\mathcal{B}_{\text{stall}}$ and $\mathcal{B}_{\text{ms}}$ extremal arcs, are given by:

$$\Delta\psi_{\mathcal{B}_{\text{min/ms}}}(\psi_i,\delta,v) = \delta \tag{36}$$

$$\Delta x_{\mathcal{B}_{\text{min/ms}}}(\psi_i,\delta,v) = \text{sgn}(\delta)\left(\frac{v(\sin(\psi_i+\delta)-\sin\psi_i)}{u_{\max}}\right) \tag{37}$$

$$\Delta y_{\mathcal{B}_{\text{min/ms}}}(\psi_i,\delta,v) = \text{sgn}(\delta)\left(\frac{v(-\cos(\psi_i+\delta)+\cos\psi_i)}{u_{\max}}\right) \tag{38}$$

$$\Delta h_{\mathcal{B}_{\text{min/ms}}}(\psi_i,\delta,v) = \frac{|\delta|(av^2+bv+c)}{u_{\max}} \tag{39}$$

B Solving for $\mathcal{BSB}$ Extremal Controls

In Appendix A individual $\mathcal{B}$ arcs and $\mathcal{S}$ segments are parametrized to give the resulting planar displacements and changes in heading resulting from each extremal control. However in a $\mathcal{BSB}$ extremal sequence, the three consecutive extremals are related by additional constraints. (For example, the final heading of a given extremal must correspond to the initial heading of the following extremal.) Let the first $\mathcal{B}$ arc begin with

heading $\psi_i = 0$ and result in a heading change $\delta = \alpha$. Recall that the $\mathcal{S}$ segment must have a heading $\psi = \theta + \pi$, thus $\alpha = \theta + \pi$. Further, if the $\mathcal{S}$ segment is of length L and the final $\mathcal{B}$ arc corresponds to a heading change $\delta = \gamma$, then the $\mathcal{BSB}$ extremal is uniquely defined. Also, for a $\mathcal{BSB}$ sequence $\lambda = v_{\text{stf}} - v_{\text{ms}}$, thus this constant is known. Hence the parameters α, L and γ are sufficient to define a $\mathcal{BSB}$ extremal and all subsets thereof. To satisfy the boundary conditions, this sequence must result in a final heading ψ_1, thus we have the constraint:

$$\begin{aligned}\psi_1 &= \Delta\psi_{\mathcal{B}}(0,\alpha,\alpha-\pi,\lambda) + \Delta\psi_{\mathcal{S}}(L,\alpha) + \Delta\psi_{\mathcal{B}}(\alpha,\alpha-\pi,\gamma,\lambda) \\ &= \alpha+\gamma \mod 2\pi \end{aligned} \tag{40}$$

Similarly, for the final planar positions x_1 and y_1

$$\begin{aligned} x_1 &= \Delta x_{\mathcal{B}}(0,\alpha,\alpha-\pi,\lambda) + \Delta x_{\mathcal{S}}(L,\alpha) + \Delta x_{\mathcal{B}}(\alpha,\alpha-\pi,\gamma,\lambda) \\ &= \frac{\lambda[\alpha c(\alpha)+s(\alpha)]+2v_{\text{ms}}s(\alpha)}{2u_{\max}}\text{sgn}(\alpha) + Lc(\alpha) \\ &\quad + \frac{\lambda[\gamma c(\alpha)+c(\alpha+\gamma)s(\gamma)]+2v_{\text{ms}}[s(\alpha+\gamma)-s(\alpha)]}{2u_{\max}}\text{sgn}(\gamma) \end{aligned} \tag{41}$$

$$\begin{aligned} y_1 &= \Delta y_{\mathcal{B}}(0,\alpha,\alpha-\pi,\lambda) + \Delta y_{\mathcal{S}}(L,\alpha) + \Delta y_{\mathcal{B}}(\alpha,\alpha-\pi,\gamma,\lambda) \\ &= \frac{\lambda\alpha s(\alpha)+2v_{\text{ms}}[1-c(\alpha)]}{2u_{\max}}\text{sgn}(\alpha) + Ls(\alpha) \\ &\quad + \frac{\frac{\lambda}{4}[c(\alpha)-c(\alpha-2(\alpha+\gamma))+2\gamma s(\alpha)]+v_{\text{ms}}[c(\alpha)-c(\alpha+\gamma)]}{u_{\max}} \\ &\qquad \text{sgn}(\gamma) \end{aligned} \tag{42}$$

where the shorthand notation $c(\cdot) = \cos(\cdot)$ and $s(\cdot) = \sin(\cdot)$ is used. The system of three equations (40)-(42) has three unknowns (α, L, γ) and can be solved with a multi-variate root finding routine. However, we may also simplify this solution procedure by transcribing the problem into a root solving problem for one parameter. One advantage of this approach is that root-finding routines, such as chebfun developed by the University of Oxford [40], are capable of reliably finding all roots of a single variable on a given interval. The system (40)-(42) can be rearranged into the form:

$$f_1(\alpha,L,\gamma)\cos\alpha + k_1\sin\alpha + k_2\sin\gamma = k_3 \tag{43}$$

$$f_1(\alpha,L,\gamma)\sin\alpha + k_4\cos\alpha + k_5\cos(\alpha+2\gamma) = k_6 \tag{44}$$

$$\alpha+\gamma \mod 2\pi = \psi_1 \tag{45}$$

where

$$f_1(\alpha,L,\gamma) = 2u_{\max}L + \lambda(|\alpha|+|\gamma|) \tag{46}$$

and the constants depend on the sign of α and γ, (corresponding to a given path orientation):

$$\begin{aligned} k_1 &= (\lambda+2v_{\text{ms}})\text{sgn}(\alpha) - 2v_{\text{ms}}\text{sgn}(\gamma) \\ k_2 &= \lambda\ \text{sgn}(\gamma)\cos\psi_1 \\ k_3 &= 2u_{\max}x_1 - 2v_{\text{ms}}\sin\psi_1\text{sgn}(\gamma) \\ k_4 &= \frac{(\lambda+4v_{\text{ms}})\text{sgn}(\gamma)}{2} - 2v_{\text{ms}}\text{sgn}(\alpha) \\ k_5 &= -\frac{\lambda\ \text{sgn}(\gamma)}{2} \\ k_6 &= 2u_{\max}y_1 - 2v_{\text{ms}}\text{sgn}(\alpha) + 2v_{\text{ms}}\cos\psi_1\text{sgn}(\gamma) \end{aligned}$$

Assume that $\cos\alpha \neq 0$ and $k_3 - k_1\sin\alpha - k_2\sin\gamma \neq 0$, and note that for any nonzero triple (α,L,γ) the term $f_1(\alpha,L,\gamma) > 0$. Then divide (44) by (43) to eliminate $f_1(\alpha,L,\gamma)$:

$$\frac{\sin\alpha}{\cos\alpha} = \frac{k_6 - k_4\cos\alpha - k_5\cos(\alpha+2\gamma)}{k_3 - k_1\sin\alpha - k_2\sin\gamma} \tag{47}$$

Using (45) the constraint (47) can be rewritten as

$$\begin{aligned} g_1(\alpha) &= \sin\alpha[k_3 - k_1\sin\alpha - k_2\sin(\psi_1-\alpha)] \\ &\quad - \cos\alpha[k_6 - k_4\cos\alpha - k_5\cos(2\psi_1-\alpha)] \\ &= 0 \end{aligned} \tag{48}$$

The roots of $g_1(\alpha)$ over the interval $\alpha \in (-2\pi, 2\pi)$ give candidate values for α, where positive roots correspond to initial left turns and negative roots to initial right turns. For each candidate α two candidate γ can be determined from (45), corresponding to a final left turn ($\gamma > 0$) or a final right turn ($\gamma < 0$). Once a candidate α and γ have been found, $f_1(\alpha,L,\gamma)$ is computed from

$$f_1(\alpha,L,\gamma) = \frac{k_3 - k_1\sin\alpha - k_2\sin\gamma}{\cos(\alpha)}$$

and, lastly, L is determined from (46).

However, if $\cos(\alpha) = 0$ or $k_3 - k_1\sin\alpha - k_2\sin\gamma = 0$, then the previous assumptions do not hold. Note that if $k_3 - k_1\sin\alpha - k_2\sin\gamma = 0$ then (43) implies that $\cos\alpha = 0$, thus both conditions are equivalent. If $\cos(\alpha) = 0$ then the candidate α are $\pm\pi/2$ or $\pm 3\pi/2$ and the solution is algebraic (we omit it here for brevity).

C Solving for $\mathcal{BBBB}$ Extremal Controls

Consider the class of $\mathcal{BBBB}$ candidate optimal controls, the first $\mathcal{B}$ arc begins with heading $\psi_i = 0$ and subtends an angle α (where the sign of the angle represents the direction of the turn). The next two $\mathcal{B}$ arcs in the sequence are anti-symmetric to each other. From Lemma 15, if the second arc subtends an angle β, then $\theta = (\alpha+\beta)/2$. Because the third arc is antisymmetric to the first, the change in heading along this $\mathcal{B}$ arc is $-\beta$. Last, the final arc subtends an angle γ. For this class and path type $\lambda \leq v_{\text{ms}} - v_{\text{stall}}$ and the parameter vector $p = (\alpha \quad \beta \quad \gamma \quad \lambda)^{\text{T}}$ uniquely defines the sequence. Note that for a given path orientation (for example, *RLRL*) the angles α, β, γ are constrained in sign and magnitude. Thus the parameters must lie in a region defined by a polytope of the form $Ap \leq b$. Using the expressions in Appendix A, a constraint for the boundary conditions can be formulated as

$$g(p) = \begin{pmatrix} x(p) - x_1 \\ y(p) - y_1 \\ \psi(p) - \psi_1 \end{pmatrix} = 0$$

where $\mathbf{x}_p = (x(p) \quad y(p) \quad \psi(p))^{\text{T}}$ is the terminal state for a given parameter vector p. Further the expressions for the change in altitude can be used to express the total cost $J(p)$. Then the constrained optimization problem is:

$$\begin{aligned} &\min J(p) \\ &\text{subject to } Ap \leq b \\ &g(p) = 0 \end{aligned} \tag{49}$$

A numerical solver, such as fmincon, developed by MATLAB [41], may return a locally optimal solution to the problem (49),

if one exists. Note that this formulation applies only to $\mathcal{BBBB}$ sequences, however shorter sequences, such as $\mathcal{BBB}$ or $\mathcal{BB}$ will have different constraints and they are not detailed here for brevity.

D Solving for $\mathcal{B}_{\text{stall}}\mathcal{B}_{\text{stall}}\mathcal{B}_{\text{stall}}\mathcal{B}_{\text{stall}}$ and $\mathcal{B}_{\text{ms}}$ Extremals

Recall that the "middle" $\mathcal{B}_{\text{stall}}$ arcs in a $\mathcal{B}_{\text{stall}}\mathcal{B}_{\text{stall}}\mathcal{B}_{\text{stall}}\mathcal{B}_{\text{stall}}$ sequence are anti-symmetric and each correspond to heading changes $|\Delta\psi| = \pi$. If the first arc in this sequence subtends an angle α, and the final arc subtends an angle γ, then the sequence is uniquely defined by these two parameters. Let $k = \text{sgn}(\alpha)$ denote the sign of initial turn (left or right). Then the boundary conditions are:

$$x_1 = \Delta x_{\mathcal{B}_{\text{stall}}}(0,\alpha) + \Delta x_{\mathcal{B}_{\text{stall}}}(\alpha,-k\pi) + \Delta x_{\mathcal{B}_{\text{stall}}}(\alpha-k\pi,k\pi) + \Delta x_{\mathcal{B}_{\text{stall}}}(\alpha,\gamma) \tag{50}$$

$$y_1 = \Delta y_{\mathcal{B}_{\text{stall}}}(0,\alpha) + \Delta y_{\mathcal{B}_{\text{stall}}}(\alpha,-k\pi) + \Delta y_{\mathcal{B}_{\text{stall}}}(\alpha-k\pi,k\pi) + \Delta y_{\mathcal{B}_{\text{stall}}}(\alpha,\gamma) \tag{51}$$

$$\psi_1 = \alpha + \gamma \tag{52}$$

Using (50) and (52), we find that

$$\sin(\alpha) = \frac{x_1 u_{\max}}{6 k v_{\text{stall}}} + \frac{\sin\psi_1}{6} \tag{53}$$

gives α, and $\gamma = \psi_1 - \alpha$. Similarly, in a $\mathcal{B}_{\text{stall}}\mathcal{B}_{\text{stall}}\mathcal{B}_{\text{stall}}$ sequence, let the initial $\mathcal{B}_{\text{stall}}$ arc subtend α the middle arc subtend $-k\pi$ and the final arc subtend γ. In this case we obtain

$$\sin(\alpha) = \frac{x_1 u_{\max}}{4 k v_{\text{stall}}} - \frac{\sin\psi_1}{4} \tag{54}$$

and $\gamma = \psi_1 - \alpha + k\pi$. Likewise, for a $\mathcal{B}_{\text{stall}}\mathcal{B}_{\text{stall}}$ sequence

$$\sin(\alpha) = \frac{x_1 u_{\max}}{2 k v_{\text{stall}}} + \frac{\sin\psi_1}{2} \tag{55}$$

and, again, $\gamma = \psi_1 - \alpha$. The case of a single $\mathcal{B}_{\text{stall}}$ or $\mathcal{B}_{\text{stall}}$ is trivial since the arc must subtend an angle equal to the final heading ψ_1.